Molecular Human Reproduction vol.6 no.12 pp. 1119–1130, 2000

Calcium influx in human uterine epithelial RL95-2 cells triggers adhesiveness for trophoblast-like cells. Model studies on signalling events during embryo implantation

Hanna Tinel[1], Hans-Werner Denker[2] and Michael Thie[2,3]

[1]Max-Planck Institut für molekulare Physiologie, D-44227 Dortmund, and [2]Institut für Anatomie, Universitätsklinikum, D-45122 Essen, Germany

[3]To whom correspondence should be addressed. E-mail: michael.thie@uni-essen.de

RL95-2 is a human uterine epithelial cell line that exhibits adhesion competence on its apical surface for trophoblast-like JAR cells. Using confocal microscopy and an adhesion assay we have found that changes in intracellular free calcium ($[Ca^{2+}]_i$) in RL95-2 cells are involved in binding of JAR spheroids. Impact of spheroids upon, and movement of spheroids across, monolayers of RL95-2 cells produced a transient increase in $[Ca^{2+}]_i$. Pretreatment of RL95-2 cells with the Ca^{2+} channel inhibitor, diltiazem, reduced the $[Ca^{2+}]_i$ increase. Interestingly, resting of JAR spheroids on RL95-2 cells caused no detectable alterations in $[Ca^{2+}]_i$ although cell–cell bonds were formed during prolonged contact. However, separation of established bonds did produce an increase in $[Ca^{2+}]_i$ which could be reduced by the Ca^{2+} channel blocker, SKF-96365, but not by diltiazem. SKF-96365 also reduced adhesion of JAR spheroids to RL95-2 cells. In all experiments, the increase in $[Ca^{2+}]_i$ was due to influx from the external medium, as it could be blocked both by removing extracellular Ca^{2+} and by nickel. These results suggest that the plasma membrane of uterine RL95-2 cells contains two types of Ca^{2+} channels that are involved in trophoblast adhesion, i.e. diltiazem-sensitive channels contributing to initiation of JAR cell binding and SKF-96365-sensitive channels participating in a feedback loop that controls the balance of bonds.

Key words: calcium influx/cell adhesion/implantation/polarized phenotype/uterine epithelium

Introduction

Cell–cell adhesion between the blastocyst and the endometrial mucosa is critical for successful implantation of mammalian embryos. During the initial phase of embryo implantation, the trophoblast of the blastocyst has to establish contact with the free surface of the uterine epithelium and to adhere there. Adhesion to an apical plasma membrane is a very unusual phenomenon, and the mechanisms involved are poorly understood (Denker, 1993).

With respect to the human uterine epithelium, apical contact formation with trophoblast cells seems to be possible only if the epithelium enters a specific functional state called receptivity which is thought to last from days 19–21 of a normal menstrual cycle (Finn and Martin, 1974; Navot *et al*., 1986; Lessey *et al*., 1995; Nikas and Psychoyos, 1997). Experimental studies in animals and data from human in-vitro implantation models have helped to shed light on features by which uterine cells may change their adhesive properties in this particular state. The starting point, i.e. the pre-receptive state, is a structurally and functionally polarized epithelial cell with distinct basal, lateral and apical plasma membrane domains. A reduction in the thickness of the glycocalyx of these cells and in cell surface charge has been observed (Murphy and Rogers, 1981; Morris and Potter, 1984). On the other hand, the biosynthesis and expression of new cell surface proteins has also been reported (Aplin, 1997; Lessey, 1998; Kirn-Safran and Carson, 1999). However, recent data suggest that, not only is the expression of apical membrane-associated molecules changed in the uterine epithelium at acquisition of receptivity, but changes in the lateral and basal sites of these cells can also be observed (Rogers and Murphy, 1992; Albers *et al*., 1995; Murphy, 1995; Nikas, 1999; Skinner *et al*., 1999). Putting all these data together, adhesion competence of the apical surface of uterine epithelial cells may be attained by changes in the structural and functional organization of these cells by partially down-regulating or destabilizing their apico–basal polarized phenotype (Denker, 1983, 1994b). Although still poorly understood, these alterations have consequences for the initiation of adhesion during embryo implantation.

A number of molecules have been proposed to contribute to the binding of trophoblast to uterine epithelium, specifically heparan sulphate proteoglycans and heparan sulphate-binding proteins (Carson *et al*., 1998), trophinin (Fukuda and Nozawa, 1999), and H-type-1 carbohydrate antigen (Illingworth and Kimber, 1999). However, little is known regarding signal transduction events that might form the reaction cascade leading to firm adhesion between trophoblast and uterine epithelium. To what extent these adhesion molecules might be involved in triggering such signalling events in the uterine epithelium is almost completely unknown. We have some preliminary evidence that rises in intracellular Ca^{2+} ($[Ca^{2+}]_i$) can be triggered mechanically via integrins that are apically located in RL95-2 cells (Thie *et al*., 1997). Furthermore, determination of binding forces using atomic force spectro-

© European Society of Human Reproduction and Embryology

scopy demonstrated that formation of strong cell–cell bonds between trophoblast and uterine epithelium might be a relatively slow process, possibly including sequential steps of bond formation (Thie *et al*., 1998). Therefore, it may be expected that a complex cascade of events is initiated at the free cell pole of uterine epithelial cells starting with signalling and culminating in the remodelling of this cell pole to allow firm adhesion of the trophoblast to take place. Some components involved in this process may contain elements regulated by Ca^{2+} ions, since Ca^{2+} is involved in many cellular signal transduction pathways, and regulation of cell adhesion by $[Ca^{2+}]_i$ has been observed in many cell systems (Clark and Brugge, 1995; Evenas *et al*., 1998). Thus, changes in the intracellular concentration of this second messenger in uterine epithelial cells might play an important role in embryo implantation.

RL95-2 (Way *et al*., 1983) is a human uterine epithelial cell line which, in contrast to other endometrial cell lines, e.g. HEC-1-A (Kuramoto *et al*., 1972) and AN3-CA (Dawe *et al*., 1964), not only lacks epithelial polarity and shows loosening of lateral borders and changes in actin-based cytoskeleton, but its apical pole also exhibits adhesive properties for trophoblast-like cells (Thie *et al*., 1995, 1996, 1997). In this respect, RL95-2 cells have proven to be useful as a cell culture model system for the receptive human uterine epithelium (e.g. Raboudi *et al*., 1992; John *et al*., 1993; Rohde and Carson, 1993; Liu *et al*., 1998). Thus, this system may provide novel insights into the complex process of human embryo implantation regulation. Therefore, using confocal microscopy and an adhesion assay, we investigated whether the initial contact of trophoblast-like JAR cells with human uterine epithelial RL95-2 cells is associated with changes in $[Ca^{2+}]_i$ in the uterine cells, and whether this signalling correlates with the adhesion competence of RL95-2 cells.

Materials and methods

Cell culture

Human endometrial carcinoma cell lines were purchased from the American Type Culture Collection (ATCC; Rockville, MD, USA), i.e. RL95-2 cells (CRL 1671; Way *et al*., 1983), HEC-1-A cells (HTB 112; Kuramoto *et al*., 1972), and AN3-CA cells (HTB 111; Dawe *et al*., 1964). For routine culture, cell lines were grown in plastic flasks at 37°C in a humidified atmosphere containing 5% CO_2. In brief, RL95-2 cells were seeded out in a 1 + 1 mixture of Dulbecco's modified Eagle's medium (DMEM) and Ham's F12 (Gibco-Life Technology, Eggenstein, Germany) supplemented with 10% fetal calf serum (FCS; Gibco), 10 mmol/l HEPES (Gibco), and 0.5 µg/ml insulin (Gibco), HEC-1-A cells in McCoy's 5A medium (Gibco) supplemented with 10% FCS, and AN3-CA cells in Eagle's minimum essential medium with Earle's salts and non-essential amino acids (Gibco) supplemented with 10% FCS. All media were additionally supplemented with penicillin (100 IU/ml; Gibco) and streptomycin (100 µg/ml; Gibco). The growth medium was changed every 2–3 days, and cells were subcultured by trypsinization (trypsin–EDTA solution; Gibco) when they became confluent.

For experiments, endometrial cell lines were cultured on coverslips. Cells were harvested by trypsinization from confluent routine cultures, counted (CASY1-Cell Counter; Schärfe System, Reutlingen, Germany), and adjusted to the desired concentration, i.e. RL95-2 700 000 cells, HEC-1-A 200 000 cells, and AN3-CA 300 000 cells each in 2.0 ml of the respective culture medium. Subsequently, the cell suspension was seeded out on poly-D-lysine-coated glass coverslips (12 mm in diameter) positioned in 4 cm^2 Falcon multiwells. Cells were grown in medium to confluent monolayers and used for experiments within 3 days after initiation of culture.

Spheroids of human JAR choriocarcinoma cells (ATCC: HTB 144; Pattillo *et al*., 1971) were used to investigate whether the contact of trophoblast-like cells to endometrial monolayers elicits changes in cell behaviour of endometrial cells. For this purpose, JAR spheroids were prepared according to a previously described procedure (John *et al*., 1993). Briefly, a suspension of 100 000 JAR cells/ml in Roswell Park Memorial Institute (RPMI) 1640 medium (Gibco), supplemented with 10% FCS and penicillin–streptomycin, was incubated on a gyratory shaker at 110 rpm obtaining multicelluar spheroids 72 h after initiation of culture.

Cell–cell adhesion assay

The adhesiveness of the free surface of endometrial cell monolayers for human JAR spheroids was measured using a centrifugal force-based adhesion assay. The adhesion assay has been described previously (John *et al*., 1993). Briefly, JAR spheroids were harvested, counted, and gently delivered onto a confluent monolayer of human endometrial cell lines grown on coverslips. For the experiment, growth medium was changed to standard solution supplemented with drugs as described below. After 60 min, spheroid adhesion to the endometrial monolayers was quantified by centrifuging coverslips (with the cell spheroid surface facing down) at 12 *g* for 5 min. Attached spheroids were counted and expressed as a percentage of the number of spheroids seeded.

Processing for electron microscopy

Endometrial cell monolayers were grown on poly-D-lysine-coated thermanox coverslips (Nunc, Napperville, IL, USA). For subsequent transmission electron microscopy, samples were rinsed twice in phosphate-buffered saline (PBS) and fixed in 2.5% glutardialdehyde in 0.1 mol/l cacodylate buffer, pH 7.4, for 30 min at room temperature, washed in cacodylate buffer, post-fixed with 1% OsO_4 in cacodylate buffer, dehydrated with ethanol and propylene oxide and embedded in epoxy resin (Cross, 1989). The embedded cells were separated from the thermanox coverslip by snap-freezing in liquid nitrogen. Ultrathin sections were mounted on 200-mesh copper grids, double-stained with uranyl acetate and lead citrate and examined with a Zeiss TEM 902A.

For scanning electron microscopy, samples were fixed in 2.5% glutardialdehyde in 0.1 mol/l cacodylate buffer, pH 7.4, for 30 min at room temperature. After repeated washings in distilled water, samples were dehydrated with ethanol and, at a critical point, dried using methanol as intermedium and carbon dioxide as drying medium. Then samples were sputtered with a conductive layer of gold and imaged with a Leo SEM 420.

Measurement of $[Ca^{2+}]_i$

Confluent monolayers of endometrial cells grown on coverslips were loaded with fluorescent Ca^{2+}-sensitive probes for 60 min at 37°C, i.e. 5 µmol/l Oregon green 488 BAPTA-1 AM and 10 µmol/l Fura-Red AM in standard solution containing 0.025% Pluronic F127. After loading, cell monolayers were rinsed and incubated in standard solution without Ca^{2+} probes for 10 min. Thereafter, monolayers were transferred into a Perspex chamber mounted on a stage of a confocal laser scanning microscope (Noran, Bruchsal, Germany). Cell fluorescence was excited by use of the 488-nm band of an argon ion

laser. The ratio of emission <580 nm and >580 nm for Oregon green 488 BAPTA-1 and Fura-Red respectively, was used to represent $[Ca^{2+}]_i$.

To study the effect of impact of JAR spheroids upon endometrial cells, spheroids being held horizontally by a glass pipette using the holding mode of a microinjector (Eppendorf, Hamburg, Germany) were lowered to and placed on the free surface of endometrial monolayers. The glass pipettes were pulled from borosilicate filament glass capillaries (Hilgenberg, Malsfeld, Germany) on a horizontal puller (Zeitz, München, Germany). The exact position of the tip of the pipette was controlled using a micromanipulator (Luigs & Neumann, Rattingen, Germany). JAR spheroids resting on endometrial monolayers were subsequently moved over the endometrial cells by pushing the holding pipette horizontally. Glass beads (250–300 μm in diameter; Braun Melsung, Melsung, Germany) were used as control. All experiments were performed at room temperature.

Solutions

The standard solution contained 118 mmol/l NaCl, 10 mmol/l Na^+-*N*-2-hydroxyethylpiperazine-*N*'-2-ethanesulphonic acid (HEPES), 10 mmol/l H^+-HEPES, 3.2 mmol/l KCl, 2.5 mmol/l $CaCl_2$, 1.8 mmol/l $MgSO_4$, 1.8 mmol/l KH_2PO_4, 5 mmol/l glucose, 10% FCS, pH 7.4. In some experiments, as specifically indicated, cells were incubated in standard solution without $CaCl_2$ and FCS (Ca^{2+}-free solution).

Inhibiting drugs (SKF-96365, Calbiochem, Bad Soden, Germany; diltiazem and nifedipin, Sigma, Deisenhofen, Germany) were dissolved first in dimethyl sulphoxide (final solvent concentration 0.1%). The cells were preincubated with these drugs in standard solution for 10 min at 37 °C. Medium containing 0.1% dimethyl sulphoxide only served as a control.

Pluronic F-127, Oregon green 488 BAPTA-1 AM, and Fura-Red AM were purchased from Molecular Probes (Eugene, OR, USA). All other chemicals were purchased from Serva (Heidelberg, Germany).

Statistical analysis

Values are presented as mean ± SE, with n denoting the number of experiments. Paired and unpaired t-tests were applied as appropriate. $P < 0.05$ was considered to be statistically significant.

Results

Effect of impact, resting and movement of JAR spheroids on the $[Ca^{2+}]_i$ of endometrial cells

Prior to adhesion and final implantation, the blastocyst initially contacts the uterine epithelium. We developed a model of blastocyst–uterus interaction in order to investigate changes in $[Ca^{2+}]_i$ of uterine epithelial cells during this phase of initial contact. We measured $[Ca^{2+}]_i$ in either RL95-2, HEC-1-A, or AN3-CA monolayer-cultured cells under three sets of conditions: (i) during impact of JAR spheroids upon monolayer-cultured cells; (ii) during rest of unmoved spheroids on the monolayers; and (iii) while spheroids were moved across the free surface of monolayers.

Impact of JAR spheroids upon monolayers of RL95-2 cells evoked a marked increase of $[Ca^{2+}]_i$. A representative reaction is shown in Figure 1A. The fluorescence ratio increased within 15 s after initial contact, reached a maximum and decreased towards the pre-contact level within 120 s. In HEC-1-A cells, this Ca^{2+} response was significantly lower (Figure 1B). The impact of spheroids on AN3-CA cells had no significant effect on the $[Ca^{2+}]_i$ (Figure 1B).

After recovery from the initial impact, subsequent resting of JAR spheroids on monolayers of RL95-2, HEC-1-A and AN3-CA cells for up to 60 min had no effect on the $[Ca^{2+}]_i$ in the endometrial cells (data not shown).

Movement of JAR spheroids across monolayers of RL95-2 cells, but not across monolayers of HEC-1-A and AN3-CA, evoked changes in $[Ca^{2+}]_i$. As shown in Figure 2A, the $[Ca^{2+}]_i$ of RL95-2 cells increased transiently throughout spheroid movement. The latency of the rise of $[Ca^{2+}]_i$ along the route of the spheroid movement (trace) was related to the speed of spheroid movement (Figure 2B). Spreading of the Ca^{2+} wave away from the area of spheroid contact (trace) was not observed during the experiment. As a control, we checked whether the increase of $[Ca^{2+}]_i$ in RL95-2 cells was based on specific cell–cell interactions or was evoked by mechanical stimulation. As an alternative to JAR spheroids, glass beads were used. Figure 3 shows the changes in $[Ca^{2+}]_i$ due to the movement of a glass bead across a RL95-2 monolayer. The pattern of the transient $[Ca^{2+}]_i$ increase caused by glass beads was similar to that of JAR spheroids. The trace of the $[Ca^{2+}]_i$ increase, however, was narrower in experiments with glass beads than in experiments with spheroids due to the more regular shape of beads.

Adhesion competence of endometrial cells for JAR spheroids

To explore whether the differences in Ca^{2+} signalling were associated with differences in adhesive properties of endometrial cell lines, we measured the adhesion competence of RL95-2, HEC-1-A, and AN3-CA monolayers for JAR spheroids using the centrifugal force-based adhesion assay. At the chosen time point of 60 min after confrontation, a high percentage of JAR spheroids (86.4 ± 0.44%; number of spheroids tested: $n = 1294$) were attached to confluent monolayers of RL95-2 cells. In comparison, JAR spheroids attached with significantly lower efficiency to HEC-1-A cells (33.8 ± 0.38%; number of spheroids tested: $n = 1089$; $P < 0.05$) and AN3-CA cells (2.4 ± 0.19%; number of spheroids tested: $n = 1174$; $P < 0.05$). In control, glass beads used instead of JAR spheroids did not attach to RL95-2, HEC-1-A or AN3-CA cells.

Attachment morphology of spheroids adhering to RL95-2 cells

We subsequently analysed RL95-2 cells in greater detail, since, in contrast to HEC-1-A and AN3-CA cells, they showed both a strong Ca^{2+} response to an impact or movement of JAR spheroids and a high rate of adhesiveness for JAR spheroids.

As shown in Figure 4, stable cell–cell bonds developed between JAR spheroids and monolayer-cultured RL95-2 cells. Figure 4 A,B show the specific attachment morphology of a JAR spheroid adhering to the RL95-2 monolayer after 60 min of contact. Morphologically, stable cell–cell adhesion is characterized by plasma membranes coming close together and running parallel for long stretches, as well as by microvillous projections interacting with each other across an irregularly formed space at a distance of ⩽100–200 nm. Formation of organized intercellular junctions is not observed in this system.

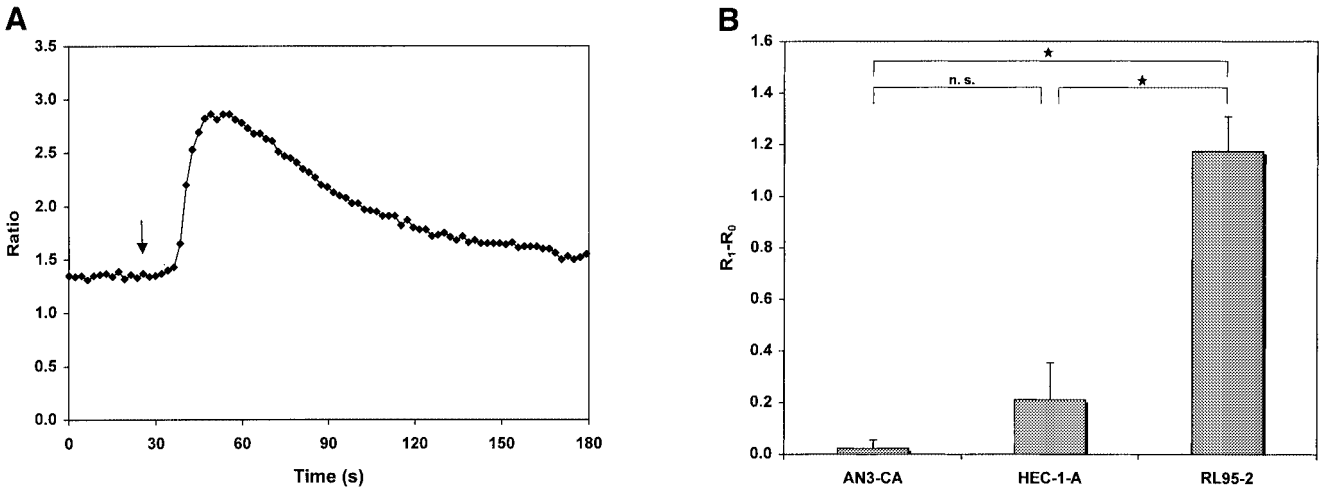

Figure 1. Changes in intracellular calcium concentration ($[Ca^{2+}]_i$) in endometrial cells during impact of JAR spheroids upon monolayers of RL95-2, HEC-1-A and AN3-CA cells. (**A**) Changes in $[Ca^{2+}]_i$ in RL95-2 cells shown as fluorescence ratio (O-green-1/Fura-Red) in a typical experiment. The arrow indicates the moment of impact of a single JAR spheroid upon the surface of a RL95-2 monolayer. (**B**) Increase in $[Ca^{2+}]_i$ in RL95-2 ($n = 4$), HEC-1-A ($n = 7$), and AN3-CA cells ($n = 6$) after impact of JAR spheroids (n = number of spheroids tested). Changes in $[Ca^{2+}]_i$ are expressed as the difference between the fluorescence ratio before (R_0) and after (R_1) impact of spheroids. *Significantly different ($P < 0.05$).

Effect of separation of cell–cell bonds between spheroids and RL95-2 cells on the $[Ca^{2+}]_i$ of RL95-2 cells

Next, we investigated whether separation of cell–cell bonds after prolonged contact between JAR spheroids and RL95-2 monolayer-cultured cells leads to Ca^{2+} signals in RL95-2 cells and whether this signal depends on the duration of cell–cell contact.

When spheroids were separated from the monolayer 10 min after contact, a transient increase of $[Ca^{2+}]_i$ was observed in the underlying RL95-2 cells. The magnitude of the Ca^{2+} rise increased continuously when the duration of contact was increased, as shown in Figure 5A. For example, the value of the maximal fluorescence ratio after 60 min of contact was 2.4-fold higher than the value after 10 min of contact. In experiments using glass beads instead of JAR spheroids, however, the magnitude of the ratio signal in RL95-2 cells was independent of the duration of contact (Figure 5B), i.e. values after 10 min of contact with a glass bead were comparable with those after 60 min of contact.

In addition, we analysed whether the duration of preceding contact of a JAR spheroid to RL95-2 cells influences the Ca^{2+} signal in RL95-2 cells along the route of subsequent spheroid movement. Figure 6 shows the values of the maximal fluorescence ratio in RL95-2 cells underlying a spheroid and in cells situated 150 μm along the route of the spheroid. While values obtained in cells of the resting area significantly increased with prolonged contact (see also above), values in cells along the trace did not. In the control, glass beads evoked increases in Ca^{2+} at the beginning of the trace similar to those observed at a distance of 150 μm. Moreover, values of maximal fluorescence ratio evoked by glass beads on their route were similar to those evoked by moving spheroids.

These experiments indicate that a rise in the Ca^{2+} signal of RL95-2 cells following detachment of JAR spheroids may be associated with separation of specific cell–cell bonds formed after prolonged spheroid contact.

Characterization of the Ca^{2+} signal in RL95-2 cells evoked by separation of cell–cell bonds between JAR spheroids and RL95-2 cells

In order to explore the source of increased $[Ca^{2+}]_i$ in the RL95-2 cells during separation of an attached JAR spheroid, we first performed experiments in Ca^{2+}-free solution (Figure 7). In the absence of Ca^{2+} in the extracellular medium, the increase of the $[Ca^{2+}]_i$ in RL95-2 cells was completely abolished. Next, we supplemented the standard solution with the Ca^{2+} channel blocker Ni^{2+} (5 mmol/l), which reduced the increase of $[Ca^{2+}]_i$ by 81.7% (Figure 7). Collectively, these data indicate that the increase of the $[Ca^{2+}]_i$ in RL95-2 cells was due to Ca^{2+} influx from the extracellular medium.

In further experiments, we characterized the nature of Ca^{2+}-channels associated with the Ca^{2+} influx in RL95-2 cells upon separation of stable cell–cell bonds. As shown above, the magnitude of the Ca^{2+} response was dependent upon the duration of contact. These data suggested that an accessory mechanism may lead to an augmentation of Ca^{2+} signalling over time. We therefore tested SKF-96365, an inhibitor of receptor-mediated Ca^{2+} channel. After 10 min of contact, the increase of $[Ca^{2+}]_i$ in the presence of SKF-96365 (100 μmol/l) did not differ significantly from the value of control. With prolonged contact, however, SKF-96365 inhibited the increase of $[Ca^{2+}]_i$ in RL95-2 cells (Figure 5A), i.e. after 20, 30, 40, 50, and 60 min of contact the increase of the value of maximal fluorescence ratio was significantly reduced by 51.1, 35.0, 40.0, 40.5, and 45.2% respectively. These results indicate that the Ca^{2+} influx induced by separation of cell–cell bonds between spheroids and RL95-2 cells consist of two components. One part of the signal is a basic Ca^{2+} influx (which is time-independent). The second part increases with the duration of contact and is probably based on receptor–ligand interactions activating a receptor-mediated Ca^{2+} channel.

As mechano-sensitive Ca^{2+} channels could be responsible

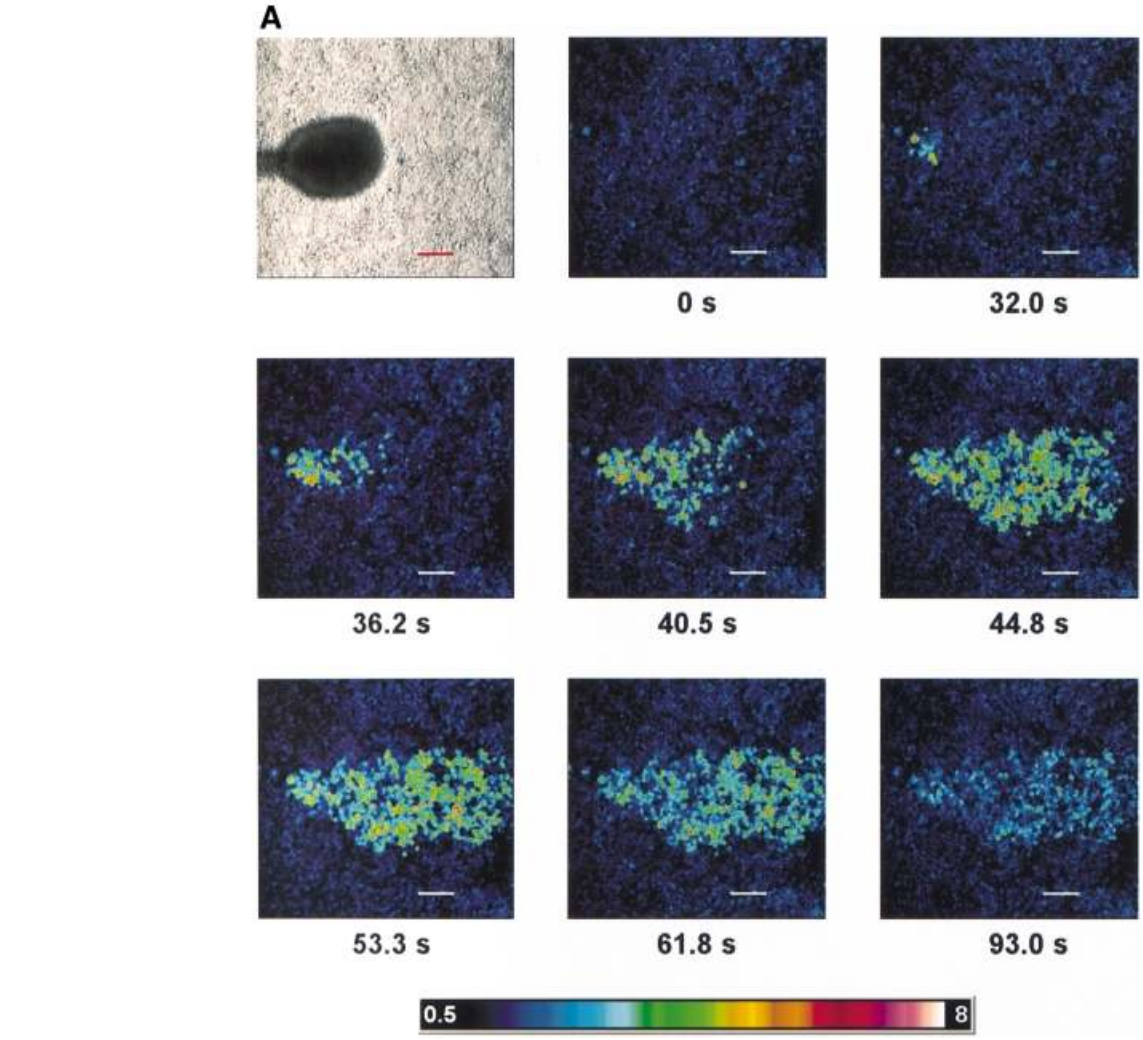

Figure 2. Changes in intracellular calcium concentration ($[Ca^{2+}]_i$) in RL95-2 cells during movement of JAR spheroids across RL95-2 monolayer. (**A**) Pseudocolour images showing changes in $[Ca^{2+}]_i$ in RL95-2 cells co-loaded with O-green-1 and Fura-Red. The first image shows a transmitted light picture of a single spheroid resting on the free surface of RL95-2 monolayer. The following fluorescence ratio images illustrate changes in $[Ca^{2+}]_i$ in the monolayer during movement of a spheroid across the monolayer after a preperiod of 20 s. Colour scale shows the fluorescence ratio range. Scale bars = 100 μm. (**B**) A typical experiment presenting changes of fluorescence ratio (O-green-1/Fura-Red) in RL95-2 cells located in the area underlying a spheroid (a), and in an area located 150 μm (b) and 300 μm (c) away from the resting area and along the route of the spheroid (trace). Arrow indicates start of spheroid movement.

for the basic part of the Ca^{2+} signal, we supplemented the incubation medium with gadolinium that is known to inhibit stretch-activated channels. However, gadolinium (500 μmol/l) showed no significant effect on the $[Ca^{2+}]_i$ increase (Figure 7). Furthermore, we tested inhibitors of voltage-gated Ca^{2+} channels, which have been reported in many epithelial cells (Zhang and O'Neil, 1999). Neither nifedipin (10 μmol/l) nor diltiazem (10 μmol/l), both well-known blockers of voltage-activated Ca^{2+}-channels, showed any effect on the Ca^{2+} response in RL95-2 cells upon separation of cell–cell bonds (Figure 7).

Characterization of the Ca^{2+} signals evoked by movement of spheroids

We also analysed the effect of Ca^{2+} channel blockers on the Ca^{2+} influx observed when spheroids were moving across the

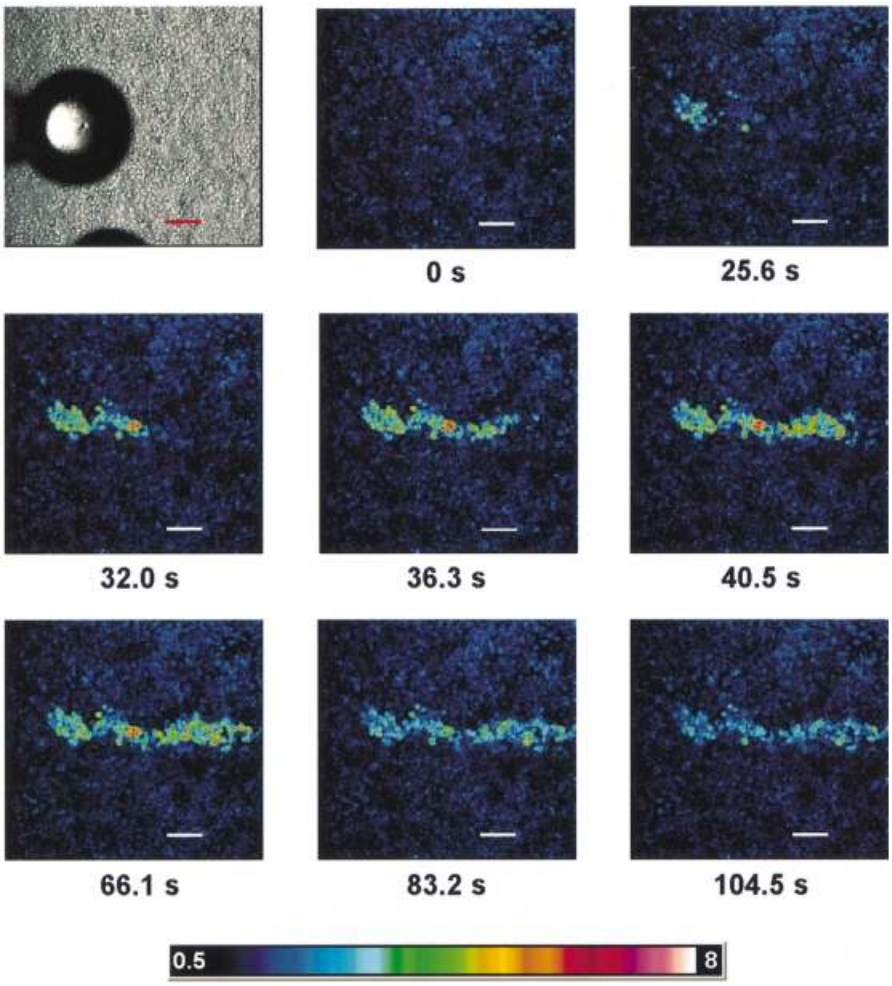

Figure 3. Changes in intracellular calcium concentration ($[Ca^{2+}]_i$) in RL95-2 cells during movement of glass beads across RL95-2 monolayer. Pseudocolor images showing changes in $[Ca^{2+}]_i$ in RL95-2 cells co-loaded with O-green-1 and Fura-Red. The first image shows a transmitted light picture of a single glass bead laying on the free surface of RL95-2 cell monolayer. The following fluorescence ratio images illustrate changes in $[Ca^{2+}]_i$ in the monolayer during movement of the glass bead across the monolayer after a preperiod of 20 s. Colour scale shows the ratio range. Scale bars = 100 μm.

surface of monolayer-cultured RL95-2 cells. While SKF-96365 (100 μmol/l) showed no significant effect on the increase of $[Ca^{2+}]_i$, diltiazem (10 μmol/l) significantly reduced the increase of $[Ca^{2+}]_i$ by 58.3% (Figure 8). Moreover, the characteristics of the Ca^{2+} channels involved in the influx in experiments with spheroid movement were similar to those observed in experiments with glass beads, i.e. gadolinium (500 μmol/l), nifedipin (10 μmol/l), and SKF-96365 (100 μmol/l) showed no effect on the increase of $[Ca^{2+}]_i$ (Figure 9), while diltiazem (10 μmol/l) again significantly reduced the Ca^{2+} response by 40.1% (Figure 5B). These results indicate that the mechanisms of Ca^{2+} influx in RL95-2 cells evoked by movement of spheroids are similar to those evoked by movement of glass beads. These mechanisms seem to be based on an activation of Ca^{2+} channels by short contact and to differ from those activated by separation of cell–cell bonds between spheroids and RL95-2 cells.

Effect of Ca^{2+}-channel blockers on adhesive properties of RL95-2 cells for JAR spheroids

We have attempted to characterize the contribution of Ca^{2+} influx to adhesive properties of RL95-2 cells for JAR spheroids by blocking the influx using Ca^{2+} channel inhibitors or by reducing the concentration of extracellular Ca^{2+} (Figure 10). In the absence of Ca^{2+}, attachment of JAR spheroids to RL95-2 cells was reduced by 97.5% when compared with standard solutions containing Ca^{2+} (adhesiveness: 2.2 ± 0.3% versus 86.4 ± 0.4%). Treatment of monolayers with Ni^{2+} (5 mmol/l) resulted in a 20.3% reduction of JAR cell attachment (adhesiveness: 68.9 ± 0.8% versus 86.4 ± 0.4%), whilst treatment with SKF-96365 (100 μmol/l) in a 7.9% reduction of attachment (adhesiveness: 79.6 ± 0.7% versus 86.4 ± 0.4%). However, treatment with diltiazem (10 μmol/l) showed no significant reduction of attachment (adhesiveness: 86.1 ± 0.5% versus 86.4 ± 0.4%) (Figure 10). No effect was observed in vehicle-treated monolayers.

Discussion

The cellular basis of interactions between trophoblast and endometrial epithelium at the beginning of embryo implantation remains poorly understood, not only with respect to the human, but even for various animal species (reviewed in

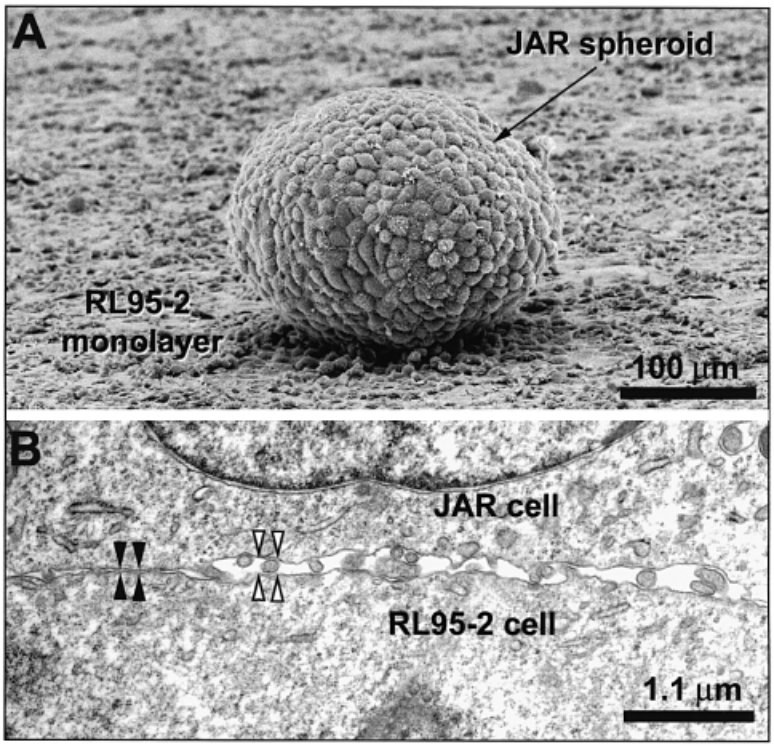

Figure 4. Attachment morphology of spheroids adhering to RL95-2 cells. (**A**) Scanning electron micrograph of a single JAR spheroid 60 min after initial contact to the free surface of a RL95-2 monolayer. (**B**) Transmission electron micrograph, corresponding to (**A**), showing how the plasma membrane of JAR cells and RL95-2 cells adhere to each other. Note the stretch of parallel, closely apposed plasma membranes (black arrows) and interacting microvillous projections (white arrows).

Denker, 1993, 1994a; Edwards, 1995; Rogers, 1995; Tabibzadeh and Babaknia, 1995; Lopata, 1996; Klentzeris, 1997). In the human, ethical and practical restraints are important obstacles in experimental studies of this aspect of reproduction. Apart from a few studies that have involved supernumerary human blastocysts obtained from IVF clinics (Lindenberg *et al*., 1986; Lindenberg, 1991; Bentin-Ley *et al*., 1999), experimental investigation has relied on model experiments using human endometrial cell lines. Among them, human uterine epithelial RL95-2 cells appear to be a useful cell culture system to investigate mechanisms driving the apical adhesiveness of uterine epithelium (Raboudi *et al*., 1992; John *et al*., 1993; Rohde and Carson, 1993; Liu *et al*., 1998). As previously shown, RL95-2 cells allow trophoblast-like JAR cells to attach to their apical pole forming strong cell–cell bonds (Thie *et al*., 1998). Additionally, we have some preliminary evidence that rises in $[Ca^{2+}]_i$ can be triggered mechanically via integrins that are apically located in RL95-2 cells (Thie *et al*., 1997). In the present study, we demonstrate that Ca^{2+} signalling is elicited in RL95-2 cells upon contact with human trophoblast-like JAR cells and that this plays a role in their subsequent binding. Although it remains unclear how this mechanism works, it seems to require the opening of at least two different types of Ca^{2+} channels in the plasma membrane of RL95-2 cells and an influx of Ca^{2+} from the extracellular fluid, transiently increasing the cytosolic Ca^{2+} concentration. Notably, Ca^{2+} release from intracellular stores in RL95-2 cells was not observed during the process of JAR cell binding.

Endometrial RL95-2 cells, but not HEC-1-A and AN3-CA cells, showed an increase of $[Ca^{2+}]_i$ upon distinct stimulation (e.g. impact or movement of JAR spheroids as well as separation of contact). This correlates with adhesion competence, features of cell architecture and expression of certain component molecules of membranes and cytoskeleton (Thie *et al*., 1995, 1997). According to these data, it appears that a particular cellular architecture as well as a molecular hierarchy of signalling pathways in RL95-2 cells enables these cells to respond to trophoblast-like cells. There is strong evidence that modulation of their epithelial phenotype, i.e. loss of apical–basal polarity, might prepare the apical cell pole for cell–cell interaction with the trophoblast. Previous studies have shown that expression of a polar phenotype, like in the case of HEC-1-A cells, prevents adhesion of trophoblast-like cells to the apical plasma membrane. However, a simple lack of cell polarity (= AN3-CA cells) of uterine cells is not sufficient to allow adhesion. Expression of adhesion molecules (e.g. α_6, β_1, β_4 integrin subunits) as well as proper organization of the cortical actin cytoskeleton, lacking in AN3-CA cells, seem to be prerequisites for binding of JAR spheroids (Thie *et al*., 1995). In this complicated network, changes in the spatial and temporal characteristics of Ca^{2+} signalling appear to be an important element in embryo–endometrium interaction.

The impact of JAR spheroids upon, and movement of spheroids across, monolayers of RL95-2 cells evoked a significant increase of $[Ca^{2+}]_i$ in RL95-2 cells. Evidence that increased $[Ca^{2+}]_i$ is due to an activation of Ca^{2+} channels came from experiments using Ca^{2+}-free solution as well as

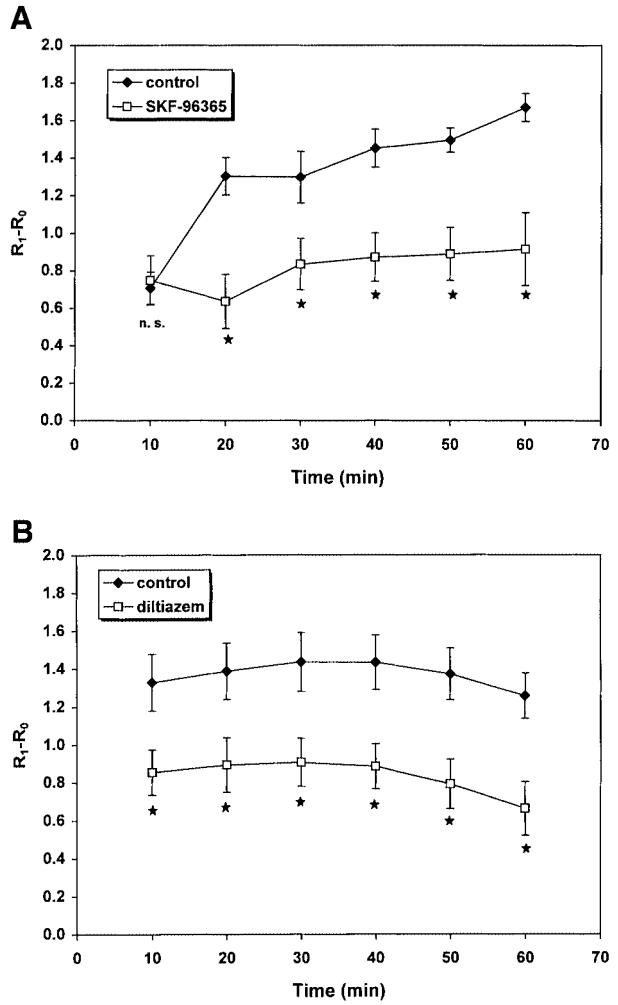

Figure 5. Effect of separation of cell–cell bonds between JAR spheroids and RL95-2 monolayers on the intracellular calcium concentration ($[Ca^{2+}]_i$) of RL95-2 cells. (**A**) Increase in $[Ca^{2+}]_i$ in RL95-2 cells upon removal of an attached JAR spheroid after a period of 10, 20, 30, 40, 50, and 60 min of cell–cell contact. Experiments were done under control conditions or in standard solution supplemented with SKF-96365 (100 µmol/l). Changes in $[Ca^{2+}]_i$ are expressed as difference between the fluorescence ratio before (R_0) and after (R_1) separation of cell–cell bonds. Values are given as mean ± SE of 6–10 separate experiments. *Significantly different ($P < 0.05$). (**B**) Increase in $[Ca^{2+}]_i$ in RL95-2 cells upon removal of a glass bead after a period of 10, 20, 30, 40, 50, and 60 min of contact. Changes in $[Ca^{2+}]_i$ are expressed as difference between the fluorescence ratio before (R_0) and after (R_1) movement of glass beads. Experiments were done under control conditions or in standard solution supplemented with diltiazem (10 µmol/l). Values are given as mean ± SE of 6–10 separate experiments. *Significantly different ($P < 0.05$).

using the divalent cation Ni^{2+} that inhibits the passage of Ca^{2+} across the channels by blocking the channel pore (Hagiwara and Byerly, 1981). In addition, increases in $[Ca^{2+}]_i$ as a result of cell damage during impact and movement of JAR spheroids across monolayers could be excluded as control experiments using monolayers of AN3-CA produced no change of $[Ca^{2+}]_i$. To characterize the types of Ca^{2+} channels involved in increases in $[Ca^{2+}]_i$, we tested the effects of various Ca^{2+} entry blockers on RL95-2 cells. The effects of diltiazem on the Ca^{2+} influx indicated that voltage-dependent Ca^{2+} channels are activated. The family of voltage-dependent Ca^{2+} channels has been described in excitable and non-excitable cells (Snutch and Reiner, 1992; Zhang and O'Neil, 1999) where they have an important role in signal transduction and Ca^{2+} transport. Diltiazem is a well-known blocker of voltage-gated L-type channels (Triggle, 1999) indicating that RL95-2 cells could posses L-type channels. However, nifedipin which is also a specific inhibitor of L-type channels (Triggle, 1999) showed no effect on the $[Ca^{2+}]_i$ in RL95-2 cells. Thus, the Ca^{2+} influx seems to occur via Ca^{2+} channels which possesses pharmacological characteristics that differ from those of the classical L-type channel. This can be correlated with the large diversity of Ca^{2+} channels due to homologous genes for different types of subunits and several types of auxiliary subunits (Mori *et al.*, 1993; Isom *et al.*, 1994).

As diltiazem blocked only a part of the Ca^{2+} signal, other types of Ca^{2+} channels appear also to be involved in gating extracellular Ca^{2+} to the interior of RL95-2 cells during short contact with JAR spheroids. Stretch-activated channels could be responsible for this effect. Mechano-sensitive Ca^{2+} channels, which are mainly involved in cell volume regulation, have been found in various types of epithelial cells (Sackin, 1995). Gadolinium is reported to block stretch-activated Ca^{2+} channels (Yang and Sachs, 1989). Although application of gadolinium showed no effect on the increase of $[Ca^{2+}]_i$ in RL95-2 cells, we cannot exclude the possibility that stretching of the plasma membrane might activate mechano-sensitive Ca^{2+} channels in RL95-2 cells, as gadolinium is not efficient in each case as has been shown in opossum kidney cells (Ubl *et al.*, 1989; Sackin, 1995). A role for receptor-mediated Ca^{2+} channels in RL95-2 cells was clearly excluded as SKF-96365, which is known to block receptor-mediated channels with high efficiency (Merritt *et al.*, 1990), did not reduce this Ca^{2+} signal in our experiments. The functional role of Ca^{2+} influx evoked by short contact with JAR spheroids requires further detailed investigation. Although diltiazem inhibited the increase of $[Ca^{2+}]_i$, it did not block the adhesiveness of JAR spheroids to RL95-2 cells. Nevertheless, complete blockade of adhesion may not necessarily be expected in such experiments. Considering that diltiazem reduced the increase of $[Ca^{2+}]_i$ in RL95-2 cells by 58.3%, the remaining level of $[Ca^{2+}]_i$ may be sufficient for JAR cell binding. Thus, having overcome repulsive interactions due to peripheral and structural features of the uterine epithelium (Thie *et al.*, 1998), activation of this Ca^{2+} signalling pathway may help to initiate attachment and adhesion of the blastocyst *in vivo*.

While short contact, e.g. impact and movement of JAR spheroids, evoked a significant increase of $[Ca^{2+}]_i$ in RL95-2 cells, further resting of spheroids on RL95-2 cells did not elicit a subsequent series of Ca^{2+} transients. This behaviour of uterine epithelial RL95-2 cells is in contrast to other cell types, e.g. vascular endothelial cells, where lymphocyte adhesion results in an oscillatory pattern of endothelial cell $[Ca^{2+}]_i$ (e.g. Pfau *et al.*, 1995; Ricard *et al.*, 1997). The reason for this difference remains to be clarified in further investigations.

The cell adhesion molecules that actually mediate trophoblast adhesion to the apical surface of uterine epithelial cells

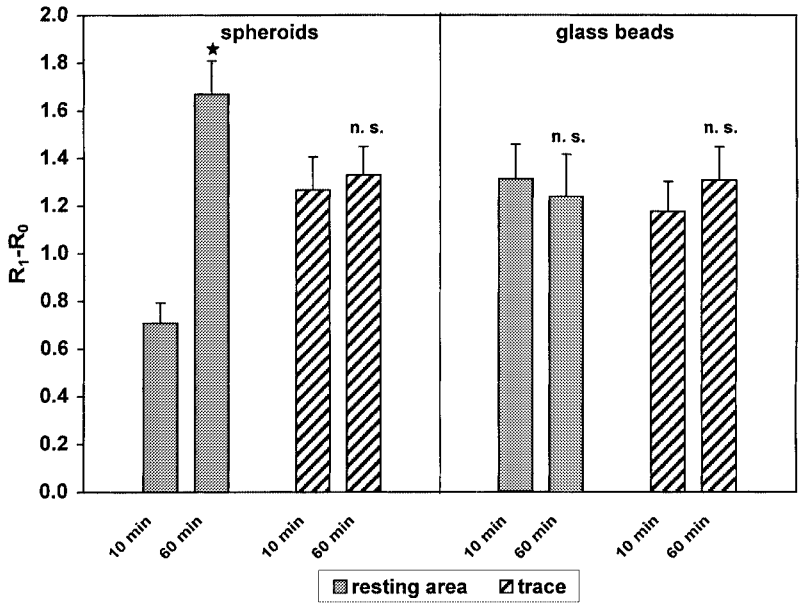

Figure 6. Comparison of changes in intracellular Ca^{2+} concentration ($[Ca^{2+}]_i$) in RL95-2 cells as evoked by separation of contact and subsequent movement of JAR spheroids compared with glass beads. Increase in $[Ca^{2+}]_i$ in RL95-2 cells located in the resting area and in an area located at a distance of 150 µm along the route of spheroids (number of spheroids tested: $n = 7$) or glass beads (number of beads tested: $n = 5$). Separation and subsequent movement was done after a period of 10 or 60 min of contact. Changes in $[Ca^{2+}]_i$ are expressed as the difference between the fluorescence ratio before (R_0) and after (R_1) separation and movement, respectively. *Significantly different, ($P < 0.05$).

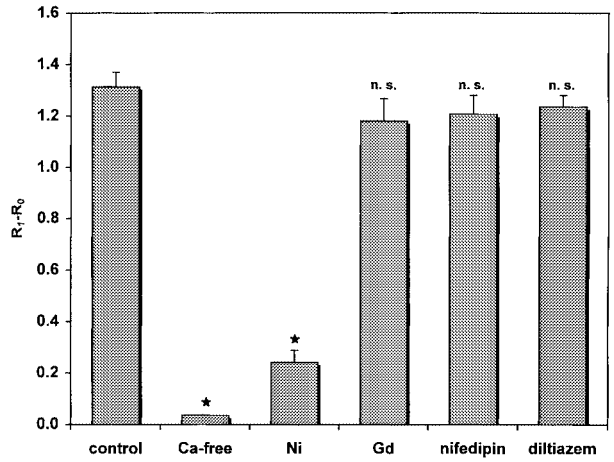

Figure 7. Effect of Ca^{2+} channel blockers and extracellular Ca^{2+} on intracellular Ca^{2+} concentration ($[Ca^{2+}]_i$) of RL95-2 cells during separation of cell–cell bonds between JAR spheroids and RL95-2 monolayers. Changes in $[Ca^{2+}]_i$ are expressed as the difference between the fluorescence ratio before (R_0) and after (R_1) separation of cell–cell bonds. Experiments were done in Ca^{2+}-free solution (number of spheroids tested: $n = 18$) or in standard solution supplemented with Ni^{2+} (5 mmol/l; $n = 24$), Gd^{3+} (500 µmol/l; $n = 18$), nifedipin (10 µmol/l; $n = 12$), or diltiazem (10 µmol/l; $n = 42$). For experiments with SKF-96365, see Figure 5A. *Significantly different ($P < 0.05$).

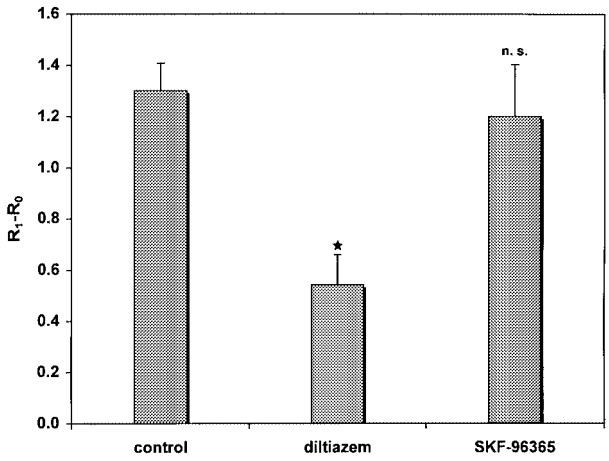

Figure 8. Effect of Ca^{2+} channel blockers on intracellular Ca^{2+} concentration ($[Ca^{2+}]_i$) of RL95-2 cells during movement of JAR spheroids across RL95-2 monolayers. Changes in $[Ca^{2+}]_i$ in RL95-2 cells located in an area 150 µm away from the resting area along the route of spheroids; changes are expressed as difference between the fluorescence ratio before (R_0) and after (R_1) movement of spheroids. Experiments were done in standard solution (number of spheroids tested: $n = 7$) or in standard solution supplemented with diltiazem (10 µmol/l; $n = 7$) or SKF-96365 (100 µmol/l; $n = 7$). *Significantly different ($P < 0.05$).

are still unknown. Various types of molecules have been proposed to play a role in this process, e.g. heparan sulphate proteoglycans and heparan sulphate-binding proteins (Carson *et al.*, 1998), trophinin (Fukuda and Nozawa, 1999), and H-type-1 carbohydrate antigen (Illingworth and Kimber, 1999). Among them, integrins have received special interest as candidate molecules potentially mediating cell–cell binding between uterine epithelium and trophoblast (Albers *et al.*, 1995; Aplin *et al.*, 1996; Bronson and Fusi, 1996; Lessey, 1998). Indeed, in RL95-2 cells, integrins, e.g. α_6, β_1, β_4 integrin subunits, are expressed along the entire plasma membrane including the free cell surface, in contrast to the non-receptive model cell line HEC-1-A, where they are missing in the apical plasma membrane (Thie *et al.*, 1995). As previously shown, mechanical stimulation of RL95-2 cells via apical membrane-

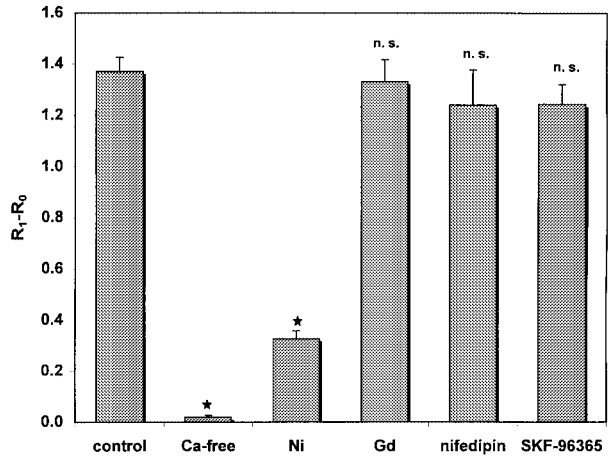

Figure 9. Effect of Ca^{2+} channel blockers and extracellular Ca^{2+} on intracellular Ca^{2+} concentration ($[Ca^{2+}]_i$) of RL95-2 cells during separation of contact between glass beads and RL95-2 monolayers. Changes in $[Ca^{2+}]_i$ are expressed as the difference between the fluorescence ratio before (R_0) and after (R_1) separation of contact. Experiments were done in Ca^{2+}-free solution (number of spheroids tested: $n = 24$) or in standard solution supplemented with Ni^{2+} (5 mmol/l; $n = 31$), Gd^{3+} (500 µmol/l; $n= 18$), nifedipin (10 µmol/l; $n = 15$), or SKF-96365 (100 µmol/l; $n = 48$). *Significantly different ($P < 0.05$).

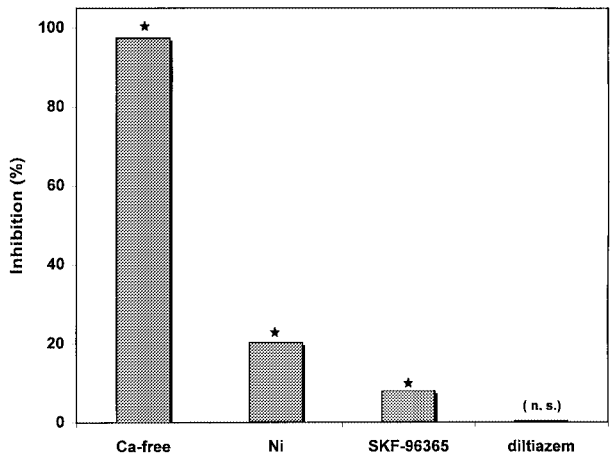

Figure 10. Effect of Ca^{2+} channel blockers and extracellular Ca^{2+} on adhesive properties of RL95-2 for JAR cells. Adhesiveness was determined in the centrifugal force-based spheroid adhesion assay. JAR spheroids were delivered onto RL95-2 monolayers in Ca^{2+}-free solution (number of spheroids tested: $n = 196$) or in standard solution supplemented with Ni^{2+} (5 mmol/l; $n = 890$), SKF-96365 (100 µmol/l; $n = 843$), or diltiazem (10 µmol/l; $n = 782$). Bars represent reduction of adhesiveness in each group of experiments. *Significantly different ($P < 0.05$).

bound integrins (using paramagnetic beads and a magnetic force drag device) can elicit a Ca^{2+} response in RL95-2 cells (Thie *et al*., 1997).

When JAR spheroids were separated from the monolayers, a transient increase in $[Ca^{2+}]_i$ was noted in the underlying RL95-2 cells. The magnitude of the Ca^{2+} rise increased continuously when the duration of contact was increased. Our data clearly show that stressing and/or separating of cell–cell bonds between uterine RL95-2 cells and trophoblast-like JAR cells activate different Ca^{2+} channels in the plasma membrane of RL95-2 cells. Our data demonstrate that the influx of Ca^{2+} may be co-regulated via receptor-mediated Ca^{2+} channels, as SKF-96365 reduced the Ca^{2+} increase up to the value observed after short contact time when bonds between the spheroid and the monolayer have not yet been established. The involvement of voltage-dependent or mechano-sensitive Ca^{2+} channels could be excluded, as neither diltiazem nor gadolinium had any effect on the increase of Ca^{2+}. The nature of receptor molecules that activate the receptor-mediated Ca^{2+} channels of uterine epithelium *in vivo* remain unknown, as the cell adhesion molecules involved in human embryo implantation have not yet been identified. As shown in other cell types, $[Ca^{2+}]_i$ can indeed play a key role in the regulation of cell–cell contacts. In the hepatocyte cell line mHepR1, $[Ca^{2+}]_i$ is necessary for the physical connection between integrins and the cytoskeleton and can link integrin signal transduction with other pathways (Nebe *et al*., 1995, 1996). In Madin-Darby Canine Kidney (MDCK) cells, integrin-mediated Ca^{2+} signalling is important in rapid feedback regulation of cell–substrate adhesion (Sjaastad *et al*., 1996). In these cells, an inositol trisphosphate (IP_3)-independent Ca^{2+} influx mechanism is responsible for integrin-mediated adhesion. The authors postulate that this Ca^{2+} influx generates Ca^{2+} gradients in the vicinity of the plasma membrane, which then modulates the adhesion processes (Sjaastad and Nelson, 1997). Similar mechanisms might regulate the adhesion of JAR spheroids. It is known that cells are able to distinguish between Ca^{2+} signals of different properties. In neurons it has been shown that a Ca^{2+}-dependent gene expression can be strengthened with Ca^{2+} concentration over a certain range (Hardingham *et al*., 1997). Thus, the amplitude of Ca^{2+} increase contains information about the magnitude of effect.

At least two different types of Ca^{2+} channels in the plasma membrane of RL95-2 cells seem to play a role in Ca^{2+} influx and activation of yet unknown Ca^{2+} sensitive response mechanisms involved in adhesiveness of uterine cells to trophoblast. One type of channel that is sensitive for diltiazem contributes to the initiation of JAR cell binding. The second channel is sensitive to SKF-96365 and participates in a feedback loop that controls the balance of bonds between uterine epithelial cells and trophoblast-like cells. Similarly, the presence of different Ca^{2+} influx mechanisms that fulfil different functions have been described in other cells. For example, neurons express both receptor-mediated and voltage-gated Ca^{2+} channels. Interestingly, the effect of Ca^{2+} entry in those cells is dependent upon the channels through which it flows. It has been shown (Bading *et al.*, 1993) that the influx of Ca^{2+} through voltage-dependent L-type channels, but not through receptor-mediated channels, activated CRE (cAMP response element)-dependent gene expression. Both types of Ca^{2+} influx could, however, activate SRE (serum response element)-dependent gene expression. With regard to uterine epithelial RL95-2 cells, cellular responses to the elevation of $[Ca^{2+}]_i$ remain a matter for further investigations.

Acknowledgements

The authors wish to thank Prof. R.K.H. Kinne (Head of the Department of Epithelial Physiology of the Max-Planck-Institute for Molecular

Physiology, Dortmund) for valuable discussions and continuous support of the project. The skilful technical assistance of Alexander Giffey, Bärbel Gobs, Birgit Maranca and Dorothea Schünke is gratefully acknowledged.

References

Albers, A., Thie, M., Hohn, H.P. *et al*. (1995) Differential expression and localization of integrins and CD44 in the membrane domains of human uterine epithelial cells during the menstrual cycle. *Acta Anat*., **153**, 12–19.

Aplin, J.D. (1997) Adhesion molecules in implantation. *Rev. Reprod.*, **2**, 84–93.

Aplin, J.D., Spanswick, C., Behzad, F. *et al*. (1996) Integrins β_5, β_3 and α_v are apically distributed in endometrial epithelium. *Mol. Hum. Reprod.*, **2**, 527–534.

Bading, H., Ginty, D.D. and Greenberg, M.E. (1993) Regulation of gene expression in hippocampal neurons by distinct calcium signaling pathways. *Science*, **260**, 181–186.

Bentin-Ley, U., Sjogren, A., Nilsson, L. *et al*. (1999) Presence of uterine pinopodes at the embryo-endometrial interface during human implantation *in vitro*. *Hum. Reprod*., **14**, 515–520.

Bronson, R.A. and Fusi, F.M. (1996) Integrins and human reproduction. *Mol. Hum. Reprod.*, **2**, 153–168.

Carson, D.D., DeSouza, M.M. and Regisford, E.G. (1998) Mucin and proteoglycan functions in embryo implantation. *Bioessays*, **20**, 577–583.

Clark, E.A. and Brugge, J.S. (1995) Integrins and signal transduction pathways: the road taken. *Science*, **268**, 233–239.

Cross, R.H.M. (1989) A reliable epoxy resin mixture and its application in routine biological transmission electron microscopy. *Micron Microsc. Acta*, **20**, 1–7.

Dawe, C.J., Banfield, W.G., Morgan, W.D. *et al*. (1964) Growth in continuous culture, and in hamsters, of cells from neoplasm associated with acanthosis nigricans. *J. Natl Cancer Inst*., **33**, 441–456.

Denker, H.-W. (1983) Basic aspects of ovoimplantation. *Obstet. Gynecol. Ann.*, **12**, 15–42.

Denker, H.-W. (1993) Implantation: a cell biological paradox. *J. Exp. Zool.*, **266**, 541–558.

Denker, H.-W. (1994a) Endometrial receptivity: cell biological aspects of an unusual epithelium. A review. *Ann. Anat.*, **176**, 53–60.

Denker, H.-W. (1994b) Cell biology of endometrial receptivity and of trophoblast–endometrial interactions. In Glasser, S.R., Mulholland, J. and Psychoyos, A. (eds), *Endocrinology of Embryo–Endometrium Interactions*. Plenum Press, New York, London, etc, pp. 17–32.

Edwards, R.G. (1995) Physiological and molecular aspects of human implantation. *Hum. Reprod*., **10**, 1–13.

Evenas, J., Malmendal, A. and Forsen, S. (1998) Calcium. *Curr. Opin. Chem. Biol*., **2**, 293–302.

Finn, C.A. and Martin, L. (1974) The control of implantation. *J. Reprod. Fertil.*, **39**, 195–206.

Fukuda, M.N. and Nozawa, S. (1999) Trophinin, tastin, and bystin: a complex mediating unique attachment between trophoblastic and endometrial epithelial cells at their respective apical cell membranes. *Semin. Reprod. Endocrinol.*, **17**, 229–234.

Hagiwara, S. and Byerly, L. (1981) Calcium channel. *Ann. Rev. Neurosc*., **4**, 69–125.

Hardingham, G.E., Chawla, S., Johnson, C.M. *et al.* (1997) Distinct functions of nuclear and cytoplasmic calcium in the control of gene expression. *Nature*, **385**, 260–265.

Illingworth, I.M. and Kimber, S.J. (1999) Demonstration of oestrogenic control of H-type-1 carbohydrate antigen in the murine endometrial epithelium by use of ICI 182,780. *J. Reprod. Fertil*., **117**, 89–95.

Isom, L.L., De Jongh, K.S. and Catterall, W.A. (1994) Auxiliary subunits of voltage-gated ion channels. *Neuron*, **12**, 1183–1194.

John, N.J., Linke, M. and Denker, H.-W. (1993) Quantitation of human choriocarcinoma spheroid attachment to uterine epithelial cell monolayers. *In Vitro Cell. Dev. Biol.*, **29A**, 461–468.

Kirn-Safran, C.B. and Carson, D.D. (1999) Dynamics of uterine glycoconjugate expression and function. *Semin. Reprod. Endocrinol*., **17**, 217–227.

Klentzeris, L.D. (1997) The role of endometrium in implantation. *Hum. Reprod.*, **12**, 170–175.

Kuramoto, H., Tamura, S. and Notake, Y. (1972) Establishment of a cell line of human endometrial adenocarcinoma *in vitro*. *Am. J. Obstet. Gynecol.*, **114**, 1012–1019.

Lessey, B.A. (1998) Endometrial integrins and the establishment of uterine receptivity. *Hum. Reprod*., **13**, 247–258.

Lessey, B.A., Castelbaum, A.J., Sawin, S.W. *et al.* (1995) Integrins as markers of uterine receptivity in women with primary unexplained infertility. *Fertil. Steril.*, **63**, 535–542.

Lindenberg, S. (1991) Experimental studies on the initial trophoblast–endometrial interaction. *Dan. Med. Bull.*, **38**, 371–380.

Lindenberg, S., Hyttel, P., Lenz, S. *et al.* (1986) Ultrastructure of the early human implantation *in vitro*. *Hum. Reprod.*, **1**, 533–538.

Liu, S., Julian, J. and Carson, D.D. (1998) A peptide sequence of heparin/heparan sulfate (HP/HS)-interacting protein supports selective, high affinity binding of HP/HS and cell attachment. *J. Biol. Chem.*, **273**, 9718–9726.

Lopata, A. (1996) Blastocyst-endometrial interaction: an appraisal of some old and new ideas. *Mol. Hum. Reprod.*, **2**, 519–525.

Merritt, J.E., Armstrong, W.P., Benham, C.D. *et al.* (1990) SKF 96365, a novel inhibitor of receptor-mediated calcium entry. *Biochem. J.*, **271**, 515–522.

Mori, Y., Niidome, T., Fujita, Y. *et al.* (1993) Molecular diversity of voltage-dependent calcium channel. *Ann. N.Y. Acad. Sci.*, **707**, 87–108.

Morris, J.E. and Potter, S.W. (1984) A comparison of developmental changes in surface charge in mouse blastocysts and uterine epithelium using DEAE beads and dextran sulfate *in vitro*. *Dev. Biol.*, **103**, 190–199.

Murphy, C.R. (1995) The cytoskeleton of uterine epithelial cells: a new player in uterine receptivity and the plasma membrane transformation. *Hum. Reprod. Update*, **1**, 567–580.

Murphy, C.R. and Rogers, A.W. (1981) Effects of ovarian hormones on cell membranes in the rat uterus. III. The surface carbohydrates at the apex of the luminal epithelium. *Cell Biophys.*, **3**, 305–320.

Navot, D., Laufer, N., Kopolovic, J. *et al.* (1986) Artifically induced endometrial cycles and establishment of pregnancies in the absence of ovaries. *N. Engl J. Med.*, **314**, 806–811.

Nebe, B., Bohn, W., Sanftleben, H. *et al.* (1996) Induction of a physical linkage between integrins and the cytoskeleton depends on intracellular calcium in an epithelial cell line. *Exp. Cell Res.*, **229**, 100–110.

Nebe, B., Rychly, J., Knopp, A. *et al.* (1995) Mechanical induction of beta 1-integrin-mediated calcium signaling in a hepatocyte cell line. *Exp. Cell Res.*, **218**, 479–484.

Nikas, G. (1999) Cell-surface morphological events relevant to human implantation. *Hum. Reprod.*, **14**, 37–44.

Nikas, G. and Psychoyos, A. (1997) Uterine pinopodes in peri-implantation human endometrium. Clinical relevance. *Ann. N.Y. Acad. Sci.*, **816**, 129–142.

Pattillo, R.A., Ruckert, A., Hussa, R. *et al.* (1971) The JAR cell line – continuous human multihormone production and controls. *In Vitro*, **6**, 398.

Pfau, S., Leitenberg, D., Rinder, H. *et al.* (1995) Lymphocyte adhesion-dependent calcium signaling in human endothelial cells. *J. Cell Biol.*, **128**, 969–978.

Raboudi, N., Julian, J., Rohde, L.H. *et al.* (1992) Identification of cell surface heparin/heparan sulfate binding proteins of a human uterine epithelial cell line (RL95). *J. Biol. Chem.*, **267**, 11930–11939.

Ricard, I., Payet, M.D. and Dupuis, G. (1997) Clustering the adhesion molecules VLA-4 (CD49d/CD29) in Jurkat T cells or VCAM-1 (CD106) in endothelial (ECV304) cells activates the phosphoinositide pathway and triggers Ca2+ mobilization. *Eur. J. Immunol.*, **27**, 1530–1538.

Rogers, P.A. (1995) Current studies on human implantation: a brief overview. *Reprod. Fertil. Dev.*, **7**, 1395–1399.

Rogers, P.A. and Murphy, C.R. (1992) Morphometric and freeze fracture studies of human endometrium during the peri-implantation period. *Reprod. Fertil. Dev.*, **4**, 265–269.

Rohde, L.H. and Carson, D.D. (1993) Heparin-like glycosaminoglycans participate in binding of a human trophoblastic cell line (JAR) to a human uterine epithelial cell line (RL95). *J. Cell. Physiol*., **155**, 185–196.

Sackin, H. (1995) Mechanosensitive channels. *Annu. Rev. Physiol.*, **57**, 333–353.

Sjaastad, M.D. and Nelson, W.J. (1997) Integrin-mediated calcium signaling and regulation of cell adhesion by intracellular calcium. *Bioessays*, **19**, 47–55.

Sjaastad, M.D., Lewis, R.S. and Nelson, W.J. (1996) Mechanisms of integrin-mediated calcium signaling in MDCK cells: regulation of adhesion by IP3- and store-independent calcium influx. *Mol. Biol. Cell*, **7**, 1025–1041.

Skinner, M.A., MacLaren, L.A. and Wildeman, A.G. (1999) Stage-dependent redistribution of the V-ATPase during bovine implantation. *J. Histochem. Cytochem.*, **47**, 1247–1254.

Snutch, T.P. and Reiner, P.B. (1992) Ca^{2+} channels: diversity of form and function. *Curr. Opin. Neurobiol.*, **2**, 247–253.

Tabibzadeh, S. and Babaknia, A., (1995) The signals and molecular pathways involved in implantation, a symbiotic interaction between blastocyst and endometrium involving adhesion and tissue invasion. *Hum. Reprod.*, **10**, 1579–1602.

Thie, M., Fuchs, P., Butz, S. *et al.* (1996) Adhesiveness of the apical surface of uterine epithelial cells: the role of junctional complex integrity. *Eur. J. Cell Biol*., **70**, 221–232.

Thie, M., Harrach-Ruprecht, B., Sauer, H. *et al.* (1995) Cell adhesion to the apical pole of epithelium: a function of cell polarity. *Eur. J. Cell Biol.*, **66**, 180–191.

Thie, M., Herter, P., Pommerenke, H. *et al.* (1997) Adhesiveness of the free surface of a human endometrial monolayer for trophoblast as related to actin cytoskeleton. *Mol. Hum. Reprod.*, **3**, 275–283.

Thie, M., Röspel, R., Dettmann, W. *et al.* (1998) Interactions between trophoblast and uterine epithelium: monitoring of adhesive forces. *Hum. Reprod*., **13**, 3211–3219.

Triggle, D.J. (1999) The pharmacology of ion channels: with particular reference to voltage-gated Ca^{2+} channels. *Eur. J. Pharmacol.*, **375**, 311–325.

Ubl, J., Murer, H. and Kolb, H.-A. (1989) Simultaneous recording of cell volume, membrane current and membrane potential: Effect of hypotonic shock. *Pfl. Arch. Eur. J. Physiol.*, **415**, 381–383.

Way, D.L., Grosso, D.S., Davis, J.R. *et al.* (1983) Characterization of a new human endometrial carcinoma (RL95-2) established in tissue culture. *In Vitro*, **19**, 147–158.

Yang, X. and Sachs, F. (1989) Block of stretch-activated ion channels in *Xenopus* oocytes by gadoliunium and calcium ions. *Science*, **243**, 1068–1071.

Zhang, M.I.N. and O'Neil, R.G. (1999) The diversity of calcium channels and their regulation in epithelial cells. *Adv. Pharmacol.*, **46**, 43–83.

Received on June 23, 2000; accepted on September 14, 2000